



Published in final edited form as:

*Methods Mol Biol.* 2010 ; 635: 207–222. doi:10.1007/978-1-60761-697-9\_15.

## Fluorescent Molecular Imaging and Dosimetry Tools in Photodynamic Therapy

Brian W. Pogue, Kimberley S. Samkoe, Summer L. Gibbs-Strauss, and Scott C. Davis

### Abstract

Measurement of fluorescence and phosphorescence in vivo is readily used to quantify the concentration of specific species that are relevant to photodynamic therapy. However, the tools to make the data quantitatively accurate vary considerably between different applications. Sampling of the signal can be done with point samples, such as specialized fiber probes or from bulk regions with either imaging or sampling, and then in broad region image-guided manner. Each of these methods is described below, the application to imaging photosensitizer uptake is discussed, and developing methods to image molecular responses to therapy are outlined.

### Keywords

Fluorescence; measurement; quantification; molecular; fluorescent; photosensitizer; imaging; instrumentation; system; fiber; spectroscopy

### 1. Introduction

Fluorescence measurements from tissue have been a part of research in photodynamic therapy for several decades, but now with the advent of increased molecular reporters, they take on some expanded roles. This chapter focuses on the methods for measurement of fluorescence and the applications of what these measurements can be used for.

The first fluorescence-based measurements of photosensitizer uptake in tissue during photodynamic therapy with Photofrin occurred more than 30 years ago (1); and at that time fluorescence measurements of tissue constituents like NADH were being sampled by UV/blue fluorescence (2). The latter studies were focused on diagnostically assessing tissue oxygenation and health with this type of sampling, and later examining response to therapy (3). Since that time, thousands of papers have examined both these areas, and in more recent times, there are very mature systems being examined for detection of dysplasia (4–6) and advanced photodynamic therapy dosimetry (7–9). While only a few clinically viable systems have been generated from all this work, there has been a widespread maturation of the technology, leading to better designs, such that optical systems can be better tailored to the constraints of particular niche areas. This maturation is very important, because the wide array of optical source, delivery systems, and detection methods can lead to considerable confusion about which optical system is optimal for which application. It is common to see competing optical technologies for niche applications where there is good commercial potential.

In the past decade there has been an explosion of work in small animal imaging, focusing on molecular imaging and reporting of tissue health, response to therapy, or presence of certain genetic or proteomic expression (10, 11). Since this time, there have been widespread commercial successes in preclinical systems for imaging, microscopy, and fluorescence sampling of tissues, allowing large growth in the areas of molecular diagnostics and

molecular medicine and therapy. In addition, commercial success in clinical applications such as surgery (12) have led the way for future use of molecular probes in tissue.

While all these developments have led to considerable excitement, it is important to recognize that the range of technologies available leads to confusion about what the term “fluorescence measurement” means. In this chapter, we take a top-level overview of what fluorescence measurement systems are available both in the commercial and in the research stages, and then examine the range of applications and commercially available probes which can be used for cancer therapy, with a particular focus on photodynamic therapy response.

## 2. Materials

The conceptual framework of the tools that can be used is shown in Fig. 15.1. The workhorse of invasive sampling, shown in Fig. 15.1a, is tissue extraction via biopsy to then liquefy and sample the fluorescence in dilute solvent. While this process has historically been the main way to proceed, there are inherent problems with this which make it less attractive for PS that tend to aggregate or those that have low fluorescent yields. Also, when the biopsy sampling will affect outcome, this method becomes problematic. The three non-invasive methods illustrated in Fig. 15.1b–e will be discussed in further detail below, as well as the strengths and limitations of each being summarized in Table 15.1.

### 2.1. Small Fiber Probe or Point Measurements

Several systems for fiber-based sampling have been developed over the years, dating back to nearly the first fluorescence measurements *in vivo* (Fig. 15.1b). Improvements in diode lasers, robust detectors for compact spectrometers and avalanche photodiodes, and filter technology have all contributed to better fluorescence detection at dramatically less expense than earlier versions. Still most advanced systems do some form of filtering or spectral fitting to the data and capture as much of the emitted spectrum as possible.

The choice of fiber diameter has a significant effect upon the signal, as previously studied (13). As the fiber size decreases below the average scattering length in tissue, the detected signal becomes one which is not significantly scattered when detected. Thus the signal is more dependent upon the scatter coefficient than anything else, but also linearly related to the fluorophore concentration. Since typical scatter length distances in tissue are near 100  $\mu\text{m}$ , then fibers larger than a few hundred microns are detecting light that is not just fluorescent but also has an inherent scatter component within it. This is not a problem, and indeed leads to higher signals, but must be interpreted carefully, because simple things like pressure on the tissue can decrease the signal due to inducing higher blood volume around the fiber tip. Changes in measurement site can also affect the signal because of local changes in tissue absorption or scattering coefficient.

There have been many interstitial studies, where the fluorescence is captured to sample the photosensitizer concentration prior to therapy. Prostate studies using this technique have been ongoing in a few sites (14).

### 2.2. Multifiber or Multipoint Model-Based Bulk Sampling

Measurement of fluorescence from larger volumes has been a goal for many researchers for over a decade (Fig. 15.1c). The most common approach to try and quantify concentrations in bulk tissue has been to model the light propagation, and use a model-based interpretation of the fluorescence to quantify the signal intensity. This approach would have the benefits of sampling the active photosensitizer concentration *in vivo* and directly sampling a large fraction of the tumor volume. Modeling is possible with either diffusion theory or Monte Carlo, where the diffusion approach is viable over larger distances with relative data (15–

20). The Monte Carlo approach is more accurate but also requires more accurate structure and optical property information to achieve this increased level of accuracy (21, 22) and because of large computational time requirements has been used mostly in smaller geometries. The most common use of this approach now is in the Caliper small animal tomography system where the IVIS 200 system (discussed in the next section) originally designed for surface imaging has added in capabilities for transmission fluorescence tomography. Similarly, the ART Inc system completes a surface scan over the animal with rasterization, and the source and detector are not collocated, so it effectively deeply samples the tissue by a millimeter or so.

Outside of small animal imaging, examples of this approach tend to be situation specific, because a clear knowledge of the tissue surface geometry are important parts of the system design. The most complete scientific design of such a system was developed for fluorescence tomography in situ to allow dosimetry of photosensitizer distribution in bulk tissues (14).

The drawbacks of this approach are obvious in that the ability to quantify heterogeneity and local changes in variation are not possible. However, the key to success in this approach is to measure the transmitted excitation signal as well as the remitted fluorescence signal, and when the normalized value of fluorescence to transmittance is used, this can match most homogeneous models with reasonable accuracy. Application of analytic or numerical diffusion theory to bulk tissue signal recovery is feasible, and could be an area of future development (20).

In vivo fluorescence molecular tomography was developed as an offshoot of these studies, as pioneered by Ntziachristos et al. (23, 24), and since that time dramatic improvements in diffuse tomography have been used to make niche systems for small animal tomography.

### 2.3. Surface Imaging

Imaging and image-guided measurement of luminescence signals are readily achieved, although mostly with customized instrumentation at this point in time (Fig. 15.1d). There has been an explosion of preclinical systems here, based upon simple broad-beam light excitation and filtered, cooled CCD detectors. Imaging systems for fluorescence of surfaces have of course been studied for many years, and endoscopically coupled systems for fluorescence bronchoscopy and laryngeal screening of malignancy have been studied extensively by Xillix Inc. (6, 25), and competing systems (26). Experimental systems for colonoscopy (27, 5), esophageal studies (28, 29), and intrasurgical use have all been developed. The intrasurgical systems have been stimulated by the approval of fluorescence guided resection techniques for Glioma tumors (12, 30, 31).

### 2.4. Image-Guided Fluorescence Sampling

It has only been within the last few years that systems have been created to test the concept of image-guided fluorescence sampling (Fig. 15.1e). This approach uses optical fibers or an imaging system embedded with or onto a standard imaging system. The goal is to provide both anatomical and fluorescent molecular information that is localized from deeper within the tissue. Imaging systems that have been combined with fluorescence are ultrasound, magnetic resonance, microCT, and optical coherence tomography. At the current time, these are largely experimental, although human studies are likely not far away. When combined with ultrasound, the fibers must be beside the transducer array, allowing either simultaneous or sequential measurement of the same volume. In the MRI, a prototype custom design for a rodent body coil was produced and tested in a 3T Philips Achieva system (32, 33). In combination with MicroCT, this has been done in a sequential manner several years ago,

and a hybrid system was recently produced to allow sequential in vivo scanning where the animal is not moved off the subject bed, but is translated directly from the MicroCT into the fluorescence tomography scanner. This process allows overlay and has been used to show the first deep tissue tomography of glioma tumor in a mouse cranium (34, 35).

### 3. Methods

#### 3.1. Small Fiber Probe or Point Measurements

Photosensitizer dosimetry is an important part of photodynamic therapy, especially considering that the interplay between the photosensitizing agent, oxygen and light is highly variable and not fully understood. Here, point measurements on the surface of a tumor are used to determine the uptake of photosensitizing drug prior to performing photodynamic therapy (Figs. 15.2 and 15.3). This is especially important in tumors with a high variability in vascular distribution, such as pancreatic cancer.

A laparotomy is performed, exposing the pancreas tumor (Panc-1 in this case) and the liver (Fig. 15.3a). The Aurora Dosimeter (Fig. 15.3b) was used to take alternating point measurements between the pancreas and liver. Pre-injection measurements, illustrated as negative time (Fig. 15.3c), are taken prior to photosensitizer injection. Verteporfin for injection (1 mg/kg) was administered via the tail vein after which measurements were immediately started and were continued for 30 min. The tumor had an immediate increase in fluorescence and then decayed slightly followed by a plateau for the duration of the 30 min. On the other hand, the liver had a more prominent increase in fluorescence but also plateaued within 5 min. A much higher signal in the liver was expected because it is part of the metabolic degradation pathway of verteporfin.

Using point measurements is a quick method of determining photosensitizer concentration within a tumor prior to PDT and allows alteration in the PDT protocol (i.e., light dose) to accommodate differences between patients for individualized therapy. The draw back to this type of measurement is that the photosensitizer concentration is highly heterogeneous within the tumor, especially in the central region that is typically necrotic. Taking surface point measurements only samples a few microns into the tissue, thus assuming that photosensitizer concentration is homogeneous throughout the entire sample.

#### 3.2. Bulk Sampling

Measuring fluorescence in vivo in a large sample of tissue can provide important information regarding the presence, general location, and changes in status of a tumor. The example presented here detects the presence of a brain tumor in a mouse using diffuse fluorescence tomography. Bulk sampling can be used as a method of non-invasive imaging to determine the presence of a tumor or stratify animals into treatment groups.

A mouse implanted with an orthotopic brain tumor (U251) was injected with LI-COR IRDye 800 CW EGF optical probe 48 h prior to imaging of the head (i.e., bulk tissue). The mouse was anesthetized and placed into a mouse holder, specifically made to image the brain, which accepts optical fibers used for tomography (Fig. 15.4a). The fibers were placed directly on the skin of the mouse in the plane of the tumor. Successive fluorescence and transmission measurements were made from the eight fibers surrounding the mouse head. A fluorescence map of the mouse head was then created using the NIRFAST reconstruction protocols (Fig. 15.4b).

In bulk measurements such as these, the presence and location of the tumor (high fluorescence to the left of the head) can be identified; however, specific information such as

delineation of the tumor border or distribution of the molecular marker within the tumor is limited due to the diffuse nature of bulk imaging.

### 3.3. Surface Imaging

Surface imaging can be used with a general photosensitizing agent, such as the aminolevulinic acid–protoporphyrin IX system in surgical brain resections, or a specific molecular probe, such as epidermal growth factor (EGF). Surface imaging can give you information regarding where a tumor is, its metabolic function, and even the success of treatment (i.e., PDT).

In this case, *ex vivo* tissue samples of a mouse brain are imaged to determine the location and growth factor status. Rat brain tumors transfected with green fluorescent protein (9L-GFP) were implanted into nude mice and allowed to develop for approximately 3 weeks. The mice were injected with EGF fluorescently labeled with the LI-COR IRDye 800CW via the tail vein 48 h prior to the experimental endpoint. The brains were removed, sliced, and imaged on the LI-COR Odyssey<sup>®</sup> Near-Infrared Imaging System (Fig. 15.5a). The brain slice was then imaged for the GFP fluorescence using the GE Healthcare Typhoon scanner (Fig. 15.5b). Both of these fluorescent images can be compared to the H&E histology section (Fig. 15.5c) taken from the surface of the brain slice. The GFP fluorescence arising directly from the tumor corresponds very closely with the H&E section; however, the EGF-IRDye is not evenly distributed across the entirety of the tumor. Instead, it appears that only the most actively growing regions on the edge of the tumor display increased epidermal growth factor levels.

One can imagine using surface measurements such as these to determine success of PDT, cancer, antibody, or combination therapies. The drawback of surface imaging is that the fluorescence profile of a tumor changes three dimensionally making multiple measurements or predictive assumptions necessary. Additionally, surface imaging is used best as an *ex vivo* technique or as an invasive surgical technique, limiting its use in fluorescence monitoring.

### 3.4. Image - Guided Fluorescence Sampling

Image-guided fluorescence sampling can provide very detailed *in vivo* information regarding tissue structure, metabolic activity, or tumor status for diagnosis or therapeutic monitoring. In this example magnetic resonance (MR)-guided near-infrared diffuse fluorescence tomography is used to assess the local distribution of growth factors within a brain tumor, thus providing more detailed information than the bulk sampling technique explored in **Section 3.2** and allowing for *in vivo* visualization complimentary to the *ex vivo* imaging described in **Section 3.3**.

A mouse implanted with an orthotopic U251 brain tumor was intravenously injected with EGF-IRDye 48 h prior to imaging. The mouse was anesthetized and placed into a small animal RF coil that accommodates optical fibers (Fig. 15.6a). MR images were collected on a 3.0T Achieva MR machine (Philips) while fluorescence and transmission data were collected simultaneous with a multi-spectral tomography system (Fig. 15.6b) [Davis, 2008 #4865]. The MR images of the mouse were subsequently segmented for the entire head, brain, gadolinium highlighting and non-highlighting regions. The fluorescence tomography images in Fig. 15.6c, d were created by using the segmented regions as spatial hard priors and spatial soft priors, respectively. These images illustrate that the distribution of fluorescently labeled growth factor is not homogeneous throughout the tumor and that the contrast enhanced regions of the MR image correlates with the actively growing region of the tumor.

The tomography image in Fig. 15.4b represents the same mouse without any spatial priors from the MR images (i.e., bulk sampling); thus, adding image guidance to the tomographic process allows information regarding the tumor to be elucidated in addition to the spatial parameters.

#### 4. Notes

The focus of this chapter has been on identifying the methods available to the researcher or clinician who has an interest in PDT. The tools are present and readily available for creation in any lab or for purchase from a number of technology vendors.

The primary application in PDT has been to quantify the PS concentration or activity in situ immediately prior to therapy. The drugs available for clinical use are several, and are summarized in Tables 15.2 and 15.3, with a focus on whether the fluorescence signal would have value in measurement or dosimetry in PDT. Some photosensitizers that have been in use for many years, such as Photofrin, are routinely assayed *ex vivo* through tissue biopsy sampling. In vivo measurement of fluorescence is complicated in this compound by having a multicomponent mixture of hematoporphyrins which have different photosensitivities, localization, and fluorescence levels (36). In addition, photobleaching of Photofrin has been shown to be complex due to the bleaching rate having more than one component, which was attributed to oxygen and non-oxygen mechanisms (37), making fluorescence signal complex to interpret for therapy efficacy quantification. Photosensitizing compounds that are more dominated by a single component, such as benzoporphyrin derivative, are easier to quantify and track with fluorescence because the signal seems to be linear with active photosensitizer and predictive of dose deposition (38). The endogenously generated drug protoporphyrin IX is known to photobleach rapidly and so sampling its fluorescence is thought to be quite important for tracking the response to therapy, and for interpreting dose rate effects, which can confound the therapy (39–43).

#### Acknowledgments

The authors would like to acknowledge important discussions with Tayyaba Hasan, Ph.D. (Harvard Medical School), Keith D. Paulsen Ph.D. (Dartmouth), Julie A. O'Hara, Ph.D. (Dartmouth), and P. Jack Hoopes, D.V.M. Ph.D. (Dartmouth), and experimental work by Timothy Monahan, M.S. (Dartmouth). This work has been funded through NIH grants P01CA84203 and R01CA109558.

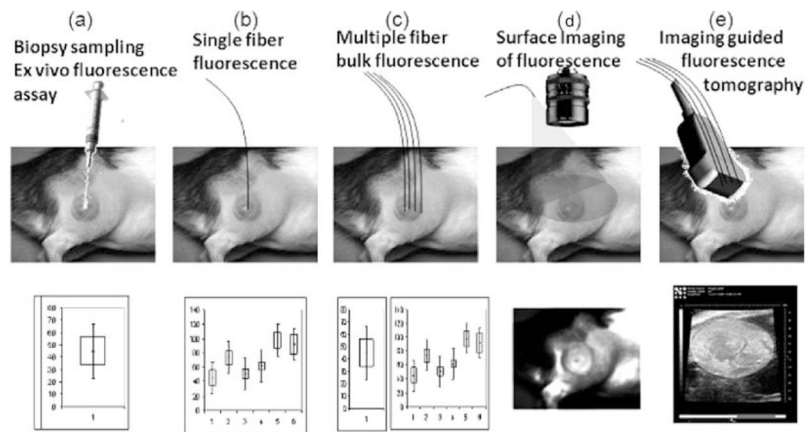
#### References

1. Kelly JF, Snell ME. Hematoporphyrin derivative: a possible aid in the diagnosis and therapy of carcinoma of the bladder. *J Urol*. 1976; 115(2):150–151. [PubMed: 1249866]
2. Ji S, Chance B, Stuart BH, Nathan R. Two-dimensional analysis of the redox state of the rat cerebral cortex in vivo by NADH fluorescence photography. *Brain Res*. 1977; 119(2):357–373. [PubMed: 187281]
3. Schantz SP, Alfano RR. Tissue autofluorescence as an intermediate endpoint in cancer chemoprevention trials. [Review]. *J Cell Biochem – Suppl*. 1993; 17F:199–204. [PubMed: 8412194]
4. Gillenwater A, Jacob R, Richards-Kortum R. Fluorescence spectroscopy: a technique with potential to improve the early detection of aerodigestive tract neoplasia. *Head Neck*. 1998; 20(6):556–562. [PubMed: 9702544]
5. DaCosta RS, Wilson BC, Marcon NE. Light-induced fluorescence endoscopy of the gastrointestinal tract. *Gastrointest Endosc Clin N Am*. 2000; 10(1):37–69. [PubMed: 10618453]
6. Weigel TL, Yousem S, Dacic S, Kosco PJ, Siegfried J, Luketich JD. Fluorescence bronchoscopic surveillance after curative surgical resection for non-small-cell lung cancer. *Ann Surg Oncol*. 2000; 7(3):176–180. [PubMed: 10791846]

7. Andersson-Engels S, Klinteberg C, Svanberg K, Svanberg S. In vivo fluorescence imaging for tissue diagnostics. *Phys Med Biol*. 1997; 42(5):815–824. [PubMed: 9172261]
8. Svanberg K, af Klinteberg C, Nilsson A, Wang I, Andersson-Engels S, Svanberg S. Laser-based spectroscopic methods in tissue characterization. *Ann N Y Acad Sci*. 1998; 838:123–129. [PubMed: 9511801]
9. Svanberg K, Wang I, Colleen S, Idvall I, Ingvar C, Rydell R, Jocham D, Diddens H, Bown S, Gregory G, Montan S, Andersson-Engels S, Svanberg S. Clinical multi-colour fluorescence imaging of malignant tumours – initial experience. *Acta Radiol*. 1998; 39(1):2–9. [PubMed: 9498864]
10. Ntziachristos V, Ripoll J, Wang LV, Weissleder R. Looking and listening to light: the evolution of whole-body photonic imaging. *Nat Biotech*. 2005; 23(3):313–320.
11. Campo MA, Lange N. Fluorescence diagnosis using enzyme-related metabolic abnormalities of neoplasia. *J Environ Pathol, Toxic Oncol*. 2006; 25(1–2):341–372.
12. Stummer W, Pichlmeier U, Meinel T, Wiestler OD, Zanella F, Reulen HJ. AL-GS Group. Fluorescence-guided surgery with 5-aminolevulinic acid for resection of malignant glioma: a randomised controlled multicentre phase III trial.[see comment]. *Lancet Oncol*. 2006; 7 (5):392–401. [PubMed: 16648043]
13. Pogue BW, Chen B, Zhou X, Hoopes PJ. Analysis of sampling volume and tissue heterogeneity upon the in vivo detection of fluorescence. *J Biomed Opt*. 2005; 10 (4):041206.
14. Finlay JC, Zhu TC, Dimofte A, Stripp D, Malkowicz SB, Busch TM, Hahn SM. Interstitial fluorescence spectroscopy in the human prostate during motexafin lutetium-mediated photodynamic therapy. *Photochem Photobiol*. 2006; 82(5):1270–1278. [PubMed: 16808592]
15. Durkin AJ, Jaikumar S, Ramanujam N, Richards-Kortum R. Relation between fluorescence spectra of dilute and turbid samples. *Appl Opt*. 1994; 33(3):414–423. [PubMed: 20862033]
16. Wu J, Feld MS, Rava RP. An analytical model for extracting intrinsic fluorescence in turbid media. *Appl Opt*. 1993; 32:3585–3595. [PubMed: 20829983]
17. Patterson MS, Pogue BW. Mathematical model for time-resolved and frequency-domain fluorescence spectroscopy in biological tissues. *Appl Opt*. 1994; 33(10):1963–1974. [PubMed: 20885531]
18. Durkin AJ, Richards-Kortum R. Comparison of methods to determine chromophore concentrations from fluorescence spectra of turbid samples. *Lasers Surg Med*. 1996; 19(1):75–89. [PubMed: 8836998]
19. Welch AJ, Gardner C, Richards-Kortum R, Chan E, Criswell G, Pfefer J, Warren S. Propagation of fluorescent light. *Lasers Surg Med*. 1997; 21(2):166–178. [PubMed: 9261794]
20. Hyde DE, Farrell TJ, Patterson MS, Wilson BC. A diffusion theory model of spatially resolved fluorescence from depth-dependent fluorophore concentrations. *Phys Med Biol*. 2001; 46(2):369–383. [PubMed: 11229720]
21. Wang, L.; Jacques, S. Monte Carlo Modeling of Light Transport in Multi-Layered Tissues in Standard C. 1992.
22. Vishwanath K, Pogue B, Mycek MA. Quantitative fluorescence lifetime spectroscopy in turbid media: comparison of theoretical, experimental and computational methods. *Phys Med Biol*. 2002; 47(18):3387–3405. [PubMed: 12375827]
23. Ntziachristos V, Bremer C, Graves EE, Ripoll J, Weissleder R. In vivo tomographic imaging of near-infrared fluorescent probes. *Mol Imaging*. 2002; 1(2):82–88. [PubMed: 12920848]
24. Ntziachristos V, Bremer C, Weissleder R. Fluorescence imaging with near-infrared light: new technological advances that enable in vivo molecular imaging. *Eur Radiol*. 2003; 13(1):195–208. [PubMed: 12541130]
25. Zargi M, Fajdiga I, Smid L. Autofluorescence imaging in the diagnosis of laryngeal cancer. *Eur Arch Oto-Rhino-Laryngol*. 2000; 257(1):17–23.
26. Zellweger M, Grosjean P, Goujon D, Monnier P, van den Bergh H, Wagnieres G. In vivo autofluorescence spectroscopy of human bronchial tissue to optimize the detection and imaging of early cancers. *J Biomed Opt*. 2001; 6(1):41–51. [PubMed: 11178579]
27. Haringsma J, Tytgat GN, Yano H, Iishi H, Tatsuta M, Ogihara T, Watanabe H, Sato N, Marcon N, Wilson BC, Cline RW. Autofluorescence endoscopy: feasibility of detection of GI neoplasms

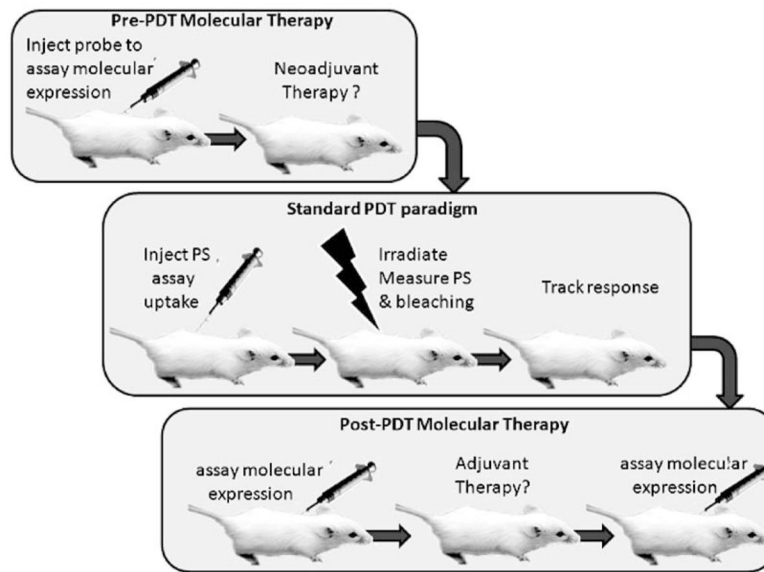
- unapparent to white light endoscopy with an evolving technology. *Gastrointest Endosc.* 2001; 53(6):642–650. [PubMed: 11323596]
28. Endlicher E, Knuechel R, Hauser T, Szeimies RM, Schölmerich J, Messmann H. Endoscopic fluorescence detection of low and high grade dysplasia in Barrett's oesophagus using systemic or local 5-aminolaevulinic acid sensitisation. *Gut.* 2001; 48(3):314–319. [PubMed: 11171819]
  29. Stepinac T, Felley C, Jornod P, Lange N, Gabrecht T, Fontollet C, Grosjean P, vanMelle G, van den Bergh H, Monnier P, Wagnieres G, Dorta G. Endoscopic fluorescence detection of intraepithelial neoplasia in Barrett's esophagus after oral administration of aminolevulinic acid. *Endoscopy.* 2003; 35(8):663–668. [PubMed: 12929061]
  30. Stummer W, Reulen HJ, Novotny A, Stepp H, Tonn JC. Fluorescence-guided resections of malignant gliomas – an overview. *Acta Neurochir –Suppl.* 2003; 88:9–12. [PubMed: 14531555]
  31. Stepp H, Beck T, Pongratz T, Meinel T, Kreth FW, Tonn JC, Stummer W. ALA and malignant glioma: fluorescence-guided resection and photodynamic treatment. *J Environ Pathol Toxic Oncol.* 2007; 26(2):157–164.
  32. Davis SC, Pogue BW, Dehghani H, Paulsen KD. Contrast-detail analysis characterizes diffuse optical fluorescence tomography image reconstruction. *J Biomed Opt.* 2005; 10(5):050501-1–3. [PubMed: 16292936]
  33. Davis SC, Springett R, Leussler C, Mazurkewitz P, Tuttle S, Gibbs-Strauss SL, Dehghani H, Pogue BW, Paulsen KD. Magnetic resonance-coupled fluorescence tomography scanner for molecular imaging of small animals and human breasts. *Rev Sci Instr.* 2008 (submitted).
  34. Kepshire D, Gibbs-Strauss SL, O'Hara JA, Hutchins M, Mincu N, Leblond F, Khayat M, Dehghani H, Srinivasan S, Pogue BW. Imaging of glioma tumor with endogenous fluorescence tomography coupled to MicroCT. *J Biomed Opt.* 2008; 14 (3):030501–030503. [PubMed: 19566285]
  35. Kepshire D, Mincu N, Hutchins M, Gruber J, Dehghani H, Hynarowski J, Leblond F, Khayat M, Pogue BW. A MicroCT guided fluorescence tomography system for small animal molecular imaging. *Rev Sci Instr.* 2009; 80:043701.
  36. Braichotte DR, Wagnieres GA, Bays R, Monnier P, van den Bergh HE. Clinical pharmacokinetic studies of photofrin by fluorescence spectroscopy in the oral cavity, the esophagus, and the bronchi. *Cancer.* 1995; 75(11):2768–2778. [PubMed: 7743484]
  37. Finlay JC, Mitra S, Patterson MS, Foster TH. Photobleaching kinetics of Photofrin in vivo and in multi-cell tumour spheroids indicate two simultaneous bleaching mechanisms. *Phys Med Biol.* 2004; 49 (21):4837–4860. [PubMed: 15584523]
  38. Zhou X, Pogue BW, Chen B, Demidenko E, Joshi R, Hoopes PJ, Hasan T. Pre-treatment photosensitizer dosimetry reduces variation in treatment response. *Int J Rad Oncol Biol Phys.* 2006; 64(4):1211–1220.
  39. Robinson DJ, de Bruijn HS, van der Veen N, Stringer MR, Brown SB, Star WM. Fluorescence photobleaching of ALA-induced protoporphyrin IX during photodynamic therapy of normal hairless mouse skin: the effect of light dose and irradiance and the resulting biological effect. *Photochem Photobiol.* 1998; 67(1):140–149. [PubMed: 9477772]
  40. Finlay JC, Conover DL, Hull EL, Foster TH. Porphyrin bleaching and PDT-induced spectral changes are irradiance dependent in ALA-sensitized normal rat skin in vivo. *Photochem Photobiol.* 2001; 73(1):54–63. [PubMed: 11202366]
  41. Star WM, Aalders MCG, Sac A, Sterenborg HJCM. Quantitative model calculation of the time-dependent protoporphyrin IX concentration in normal human epidermis after delivery of ALA by passive topical application or iontophoresis. *Photochem Photobiol.* 2002; 75(4):424–432. [PubMed: 12003134]
  42. Boere IA, Robinson DJ, de Bruijn HS, Kluijn J, Tilanus HW, Sterenborg HJCM, de Bruin RWF. Protoporphyrin IX fluorescence photobleaching and the response of rat Barrett's esophagus following 5-aminolevulinic acid photodynamic therapy. *Photochem Photobiol.* 2006; 82(6):1638–1644. [PubMed: 16879035]
  43. Sheng C, Hoopes PJ, Hasan T, Pogue BW. Photobleaching-based dosimetry predicts deposited dose in ALA-PpIX PDT of Rodent Esophagus. *Photochem Photobiol.* 2007; 83:738–748. [PubMed: 17576383]

44. Ramponi, R.; Sacchi, CA.; Cubeddu, R. Present status of research on hematoporphyrin derivatives and their photophysical properties. In: Wolbarsht, ML., editor. *Laser Applications in Medicine*. New York: Springer; 1991.
45. Brancalion L, Moseley H. Effects of photoproducts on the binding properties of protoporphyrin IX to proteins. *Biophys Chem*. 2002; 96(1):77–87. [PubMed: 11975994]
46. Aveline B, Hasan T, Redmond RW. Photophysical and photosensitizing properties of benzoporphyrin derivative monoacid ring A (BPD-MA). *Photochem Photobiol*. 1994; 59(3):328–335. [PubMed: 8016212]
47. Aveline BM, Hasan T, Redmond RW. The effects of aggregation, protein binding and cellular incorporation on the photophysical properties of benzoporphyrin derivative monoacid ring A (BPDMA). *J Photochem Photobiol B Biol*. 1995; 30(2–3):161–169.
48. Ma LW, Moan J, Berg K. Evaluation of a new photosensitizer, mesotetra-hydroxyphenyl-chlorin, for use in photodynamic therapy – a comparison of its photobiological properties with those of 2 other photosensitizers. *Int J Cancer*. 1994; 57(6):883–888. [PubMed: 8206681]
49. Glanzmann T, Hadjur C, Zellweger M, Grosiean P, Forrer M, Ballini JP, Monnier P, van den Bergh H, Lim CK, Wagnieres G. Pharmacokinetics of tetra(m-hydroxyphenyl)chlorin in human plasma and individualized light dosimetry in photodynamic therapy. *Photochem Photobiol*. 1998; 67 (5):596–602. [PubMed: 9613244]
50. Borle F, Radu A, Monnier P, van den Bergh H, Wagnieres G. Evaluation of the photosensitizer Tookad (R) for photodynamic therapy on the Syrian golden hamster cheek pouch model: Light dose, drug dose and drug-light interval effects. *Photochem Photobiol*. 2003; 78(4):377–383. [PubMed: 14626666]
51. Koudinova NV, Pinthus JH, Brandis A, Brenner O, Bendel P, Ramon J, Eshhar Z, Scherz A, Salomon Y. Photodynamic therapy with Pd-Bacteriopheophorbide (TOOKAD): successful in vivo treatment of human prostatic small cell carcinoma xenografts. *Int J Cancer*. 2003; 104(6):782–789. [PubMed: 12640688]



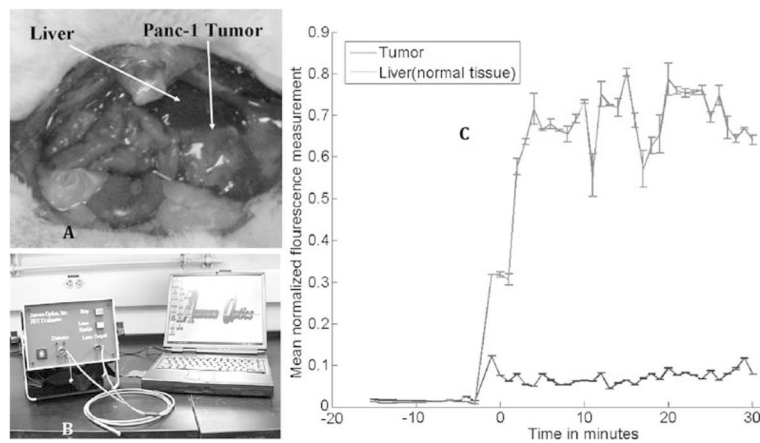
**Fig. 15.1.**

Illustration of the four methods of sampling fluorescence discussed here, including (a) the routine biopsy/tissue extraction approach; (b) the use of a single fiber probe; (c) the use of multiple fibers to sample bulk tissue; (d) surface imaging using a broad beam source and sensitive CCD imager; and (e) the concept of image-guided fluorescence quantification as applied to surface or sub-surface imaging.



**Fig. 15.2.**

The regimes in which fluorescence signals might need to be measured can be thought of as pre-PDT where neoadjuvant therapy may be beneficial based upon a measurement of the tumor molecular signals. Then during PDT, there is a clear need for PS dosimetry and possibly photobleaching dosimetry if significant. Then after PDT, adjuvant therapies are typically required, and again may be chosen based upon molecular expression, which could be measured via fluorescent probes.



**Fig. 15.3.**

Surface point measurements are used for the determination of photosensitizer concentration within a tumor allowing for individualized PDT protocol development. (a) An example of a laparotomy performed to expose the Panc-1 orthotopic pancreas tumor and liver, the two organs measured in this example. (b) The Aurora dosimeter uses blue light (405 nm) for excitation and contains a 600 nm long pass filter for fluorescence detection. The probe is made from fiber bundle containing a single illuminating fiber, surrounded by six collection fibers. The probe is directly placed against the organ of interest with moderate pressure. (c) The fluorescence of the tumor and liver are measured after injection of verteporfin (1 mg/kg). This graph is an average of four mice.

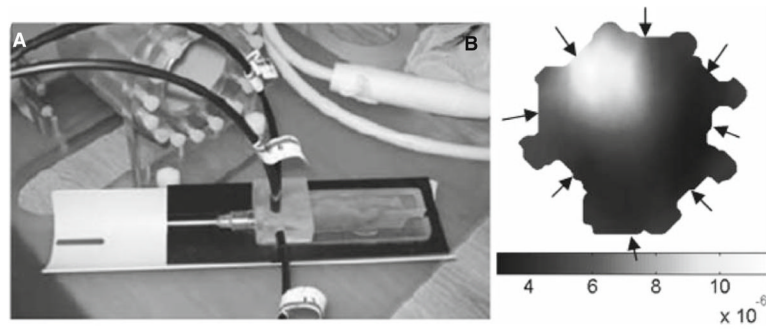


**Fig. 15.4.**

Bulk fluorescence measurements to determine the presence and location of a tumor can be performed with diffuse fluorescence tomography. In this photograph at *left*, the fibers are inserted into a mouse holding apparatus, and fluorescence transmission data is accumulated between fibers, allowing estimation with diffusion theory of the fluorescence signal origin, as shown in the diffuse tomography reconstruction at *right*. This is the fluorescence from a tracer agent localized within the glioma tumor of a mouse model (shown further in Fig. 15.6).

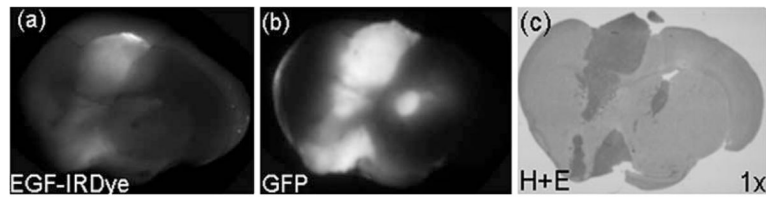


**Fig. 15.5.**

Tumor status can be determined using surface imaging of a fluorescence molecular marker. In this case, growth factor levels within an orthotopic brain tumor in a mouse can be determined ex vivo by scanning for EGF-IRDye (a) that was injected 48 h prior to killing. The tissue sample can then be scanned for GFP fluorescence to identify the entire tumor (b). The location of the tumor is confirmed with H&E staining of a fixed tissue slice taken directly from the surface of the slice imaged. The GFP and H&E images correlate very well, while the EGF molecular marker indicates areas of growth.

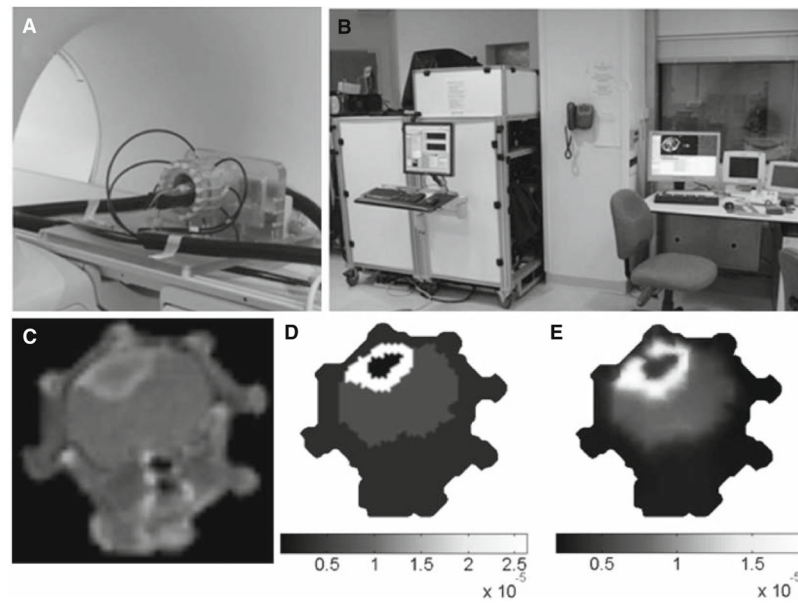


**Fig. 15.6.** Magnetic resonance (MR)-guided near-infrared diffuse optical tomography is used to illustrate how functional information can be obtained *in vivo*. A specially designed small animal RF coil accommodates optical fibers (a) so that fluorescence tomography can be performed simultaneously with MR imaging (b) (33). A T1-weighted gadolinium enhanced MR image (c) of a mouse with a U251 brain tumor is depicted. The corresponding fluorescence tomography images are illustrated in d and e using the image segmentation as spatial hard and soft priors, respectively.

**Table 15.1**

Listing of photosensitizer quantification methodologies based upon fluorescence

Methods to quantify PS	Limitations	Strengths
Tissue extraction and assay fluorescence in solution	<ul style="list-style-type: none"> <li>• Volumetric errors in handling</li> <li>• Single time point sampling</li> </ul>	<ul style="list-style-type: none"> <li>• Direct measurement of tissue</li> <li>• Most established</li> <li>• Single time point only</li> <li>• Limited ability for multiple points</li> </ul>
Point fluorescence in vivo	<ul style="list-style-type: none"> <li>• Sample individual points only</li> <li>• Insertion of fibers sometimes needed</li> <li>• Multipoint sampling takes time</li> </ul>	<ul style="list-style-type: none"> <li>• In vivo</li> <li>• Potentially real time, multi-point sampling possible</li> <li>• Track photobleaching in situ</li> </ul>
Bulk fluorescence assay in vivo	<ul style="list-style-type: none"> <li>• Non-linearity from tissue-fiber geometry</li> <li>• Model-based interpretation of data</li> </ul>	<ul style="list-style-type: none"> <li>• Obtain whole organ data</li> <li>• Thick tissue sampling</li> <li>• Direct measure during therapy</li> <li>• Integrate with online dosimetry</li> </ul>
Surface imaging of fluorescence	<ul style="list-style-type: none"> <li>• Non-linearity of signal from geometry and tissue properties</li> <li>• Limited penetration of signal</li> <li>• Surface weighted</li> <li>• Higher cost</li> </ul>	<ul style="list-style-type: none"> <li>• Several commercial systems</li> <li>• Ease of use</li> <li>• Intuitive image display</li> <li>• Fast</li> <li>• Multiple point data (surface)</li> </ul>
Image-guided fluorescence sampling	<ul style="list-style-type: none"> <li>• Non-linearity from geometry</li> <li>• Model-based interpretation</li> <li>• Imaging system required</li> <li>• Higher cost</li> </ul>	<ul style="list-style-type: none"> <li>• Obtain whole animal/ organ data</li> <li>• Thick tissue sampling</li> <li>• Visualize anatomy with signal</li> <li>• Integration into clinical workflow</li> </ul>

**Table 15.2**

Photosensitizers used in clinical PDT and their needs in terms of fluorescence dosimetry

Generic name and photosensitizer name	Fluorescence signal	Photobleaching important?	Excitation/emission
Photofrin, hematoporphyrin derivative	<ul style="list-style-type: none"> <li>Should be measured</li> <li>Permeability limited delivery</li> </ul>	<ul style="list-style-type: none"> <li>Likely important</li> </ul>	<ul style="list-style-type: none"> <li>Soret 350–420 nm</li> <li>Q-band 625–640 nm</li> <li>Emission 600–700 nm</li> <li>Reference (44)</li> </ul>
Levulnaln, aminolevulinic acid, inducing protoporphyrin IX	<ul style="list-style-type: none"> <li>Needs to be measured</li> <li>Variable production between tumors.</li> </ul>	<ul style="list-style-type: none"> <li>Critically important</li> </ul>	<ul style="list-style-type: none"> <li>Soret 400–440 nm</li> <li>Q-band 630–640 nm</li> <li>Emission 620–720 nm</li> <li>Reference (45)</li> </ul>
Verteporfin, benzoporphyrin derivative	<ul style="list-style-type: none"> <li>Needs to be measured</li> <li>Permeability limited delivery</li> </ul>	<ul style="list-style-type: none"> <li>Not clear how important</li> </ul>	<ul style="list-style-type: none"> <li>Soret 400–440 nm</li> <li>Q-band 680–695 nm</li> <li>Emission 690–705 nm</li> <li>References (46, 47)</li> </ul>
Foscan, mTHPC	<ul style="list-style-type: none"> <li>Complex fluorescence in vivo</li> <li>Permeability limited delivery</li> </ul>	<ul style="list-style-type: none"> <li>Not clear how important</li> </ul>	<ul style="list-style-type: none"> <li>Soret 380–440 nm</li> <li>Q-band 645–660 nm</li> <li>References (48, 49)</li> </ul>
WST11	<ul style="list-style-type: none"> <li>May not need to be measured</li> <li>Vascular therapy only</li> </ul>	<ul style="list-style-type: none"> <li>Not likely important</li> </ul>	<ul style="list-style-type: none"> <li>Q-band 755–770 nm</li> <li>References (50, 51)</li> </ul>

**Table 15.3**

General classes of fluorescent reporters and their uses available

<b>Molecular probes</b>	<b>Example names</b>	<b>Companies</b>
Blood flow/vascular	<ul style="list-style-type: none"> <li>• Fluorescein</li> <li>• Indocyanine Green</li> </ul>	<ul style="list-style-type: none"> <li>• Akorn Inc.</li> <li>• Sigma-Aldrich</li> </ul>
Vascular permeability	<ul style="list-style-type: none"> <li>• Methylene blue</li> <li>• Varying sized dextran bound with fluorophore</li> </ul>	<ul style="list-style-type: none"> <li>• Sigma</li> <li>• Invitrogen</li> </ul>
Receptor/ligand binding	<ul style="list-style-type: none"> <li>• Monoclonal antibodies</li> <li>• Antibody fragments</li> <li>• Peptides</li> <li>• Deoxyglucose</li> </ul>	<ul style="list-style-type: none"> <li>• Invitrogen</li> <li>• LI-COR</li> </ul>
Transfection-based reporters	<ul style="list-style-type: none"> <li>• Bioluminescence reporters</li> <li>• Fluorescent proteins</li> </ul>	<ul style="list-style-type: none"> <li>• Caliper Biosciences</li> <li>• Anticancer Inc.</li> <li>• Promega</li> </ul>
Activatable probes	<ul style="list-style-type: none"> <li>• Activated by cathepsin, matrix metalloprotease,</li> </ul>	<ul style="list-style-type: none"> <li>• VisEn Inc.</li> </ul>